

AGRÉGATS COMME PRÉCURSEURS DES NANO-OBJETS *CLUSTERS AS PRECURSORS OF NANO-OBJECTS*

Multiply charged clusters

Olof Echt ^a, Paul Scheier ^b, Tilmann D. Märk ^{b*}

^a Department of Physics, University of New Hampshire, Durham, NH 03824, USA

^b Institut für Ionenphysik, Leopold Franzens Universität, Technikerstr. 25, A-6020 Innsbruck, Austria

Received 18 March 2002; accepted 2 April 2002

Note presented by Guy Laval.

Abstract

We review progress made in understanding Coulomb explosion of multiply charged atomic clusters. Their collision with highly charged atomic ions leads to clusters in charge states as high as $z = 10$ with little vibrational excess energy; these systems approach the Rayleigh limit. Phase transitions become evident at higher excess energies. Numerous studies have been devoted to C_{60}^{z+} , like collisions with surfaces, multi-coincidence fragmentation analysis and gas-phase reactions. Stability and decay of highly charged micrometer-sized droplets and of metal di- and trianions have been monitored in ion traps. Excitation by femtosecond laser pulses allows to unravel properties of highly charged transient cluster ions. *To cite this article:* O. Echt et al., *C. R. Physique 3 (2002) 353–364*. © 2002 Académie des sciences/Éditions scientifiques et médicales Elsevier SAS

Agrégats multichargés

Résumé

Cet article présente une revue des progrès obtenus dans la compréhension de l'explosion coulombienne des agrégats atomiques multichargés. Leur collision avec des ions atomiques hautement chargés conduit à des agrégats d'état de charge aussi élevé que $z = 10$ et contenant un peu d'énergie vibrationnelle en excès. Ces systèmes approchent la limite de Rayleigh. Des transitions de phase apparaissent de manière évidente pour des excès d'énergie plus élevés. De nombreuses études ont été consacrées aux C_{60}^{z+} , concernant par exemple les collisions avec des surfaces, ou bien l'analyse en multicoïncidence de la fragmentation, ou encore les réactions en phase gazeuse. La stabilité et la décroissance de micro-gouttes hautement chargées et d'agrégats métalliques deux et trois fois négativement chargés ont été examinées dans un piège à ions. L'excitation par lasers femtosecondes permet de différencier les propriétés de ces agrégats ionisés hautement chargés. *Pour citer cet article :* O. Echt et al., *C. R. Physique 3 (2002) 353–364*. © 2002 Académie des sciences/Éditions scientifiques et médicales Elsevier SAS

* Correspondence and reprints.

E-mail addresses: olof.echt@unh.edu (O. Echt); paul.scheier@uibk.ac.at (P. Scheier); tilmann.maerk@uibk.ac.at (T.D. Märk).

1. Introduction

Highly charged droplets will become unstable with respect to charge separation when the repulsive Coulomb forces exceed a certain limit. According to Rayleigh [1], the stability limit occurs when a spherical droplet becomes unstable with respect to quadrupolar deformation; this happens when its Coulomb energy E_{Coul} exceeds twice its surface energy E_{surf} . The ratio of these quantities is called the fissility parameter X ,

$$X = \frac{E_{\text{Coul}}}{2E_{\text{surf}}} = \frac{1}{2} \frac{Q^2/8\pi\epsilon_0 r}{4\pi r^2 \gamma} = \frac{Q^2}{64\pi^2 \gamma \epsilon_0 r^3} \quad (1)$$

Here, Q is the net charge of the droplet, γ the surface tension coefficient, and r the droplet radius. When X reaches the value of 1, the droplet will ‘throw out liquid in fine jets whose fineness, however, has a limit’ [1].

One of the fascinating aspects of Coulomb instability is that it can be observed on a wide range of different length scales, from macroscopic droplets to positively or negatively charged atomic cluster ions to atomic nuclei. Atomic clusters A_n^z are usually characterized in terms of the number of building blocks n , and their net charge ze with e the elementary charge. Hence, in contrast to nuclear systems for which size and charge are closely coupled, atomic clusters offer the possibility of approaching the Rayleigh limit by either increasing the charge z for a given size n , or by reducing the size n for a given charge z .

Some questions that one may want to address are:

- Does $X = 1$ correctly mark the transition from stable to unstable clusters?
- How many fragments are being emitted?
- What is their size and charge?
- What is their kinetic energy?
- What is the effect of finite cluster temperature on the disintegration?
- If disintegration is thermally activated, what is the activation, or fission barrier?

In experiments on free atomic clusters, most of these questions can be addressed by mass and energy spectrometry, except for difficulties in measuring or controlling the cluster temperature. Any reaction in which at least two of the fragments are charged is usually called ‘fission’, or ‘Coulomb explosion’. The latter term refers to the fact that charged fragments will be accelerated in their mutual electric field when they have separated past the fission barrier.

One of the first mass spectrometric observations of the consequence of Coulomb explosion was the occurrence of a lower size limit, often called ‘critical size’ or ‘appearance size’, in mass spectra of doubly charged Xe, Pb and NaI clusters [2]. For example, the smallest size that was observed for Xe_n^{2+} was $n_{\text{app}} = 53$. Appearance sizes were often found to be nearly independent of experimental conditions but, as discussed further below, that does not imply that they mark the size where the fissility parameter reaches a value of 1. In the 1980s and early 1990s, a wealth of experimental and theoretical studies were published that investigated, e.g., the dependence of appearance sizes on the charge state, the ionization thresholds for formation of multiply charged clusters from neutral precursors and their dependence on size n , the ionization mechanism, and the size distribution of charged fragments that result from Coulomb explosion. A comprehensive review of this early work, published prior to 1992, is available [3].

Since then, a number of new approaches have been introduced that provide more detailed understanding of the energetics and dynamics of multiply charged clusters near the Rayleigh limit: they have been prepared by collisions with fast, highly charged atomic ions, or by irradiation with ultrashort laser pulses. Fullerenes have been formed in charge states up to $z = 10+$. Sophisticated mass spectrometric techniques have made it possible to monitor unimolecular (spontaneous) and induced decomposition channels in more detail. Doubly or even triply charged cluster anions have been prepared. A plethora of theoretical methods have been applied to study the fission dynamics and thermodynamics of clusters. The present review will provide a summary of these and other developments during the past 5 to 10 years. However, within the limited space we cannot accomplish more than just to mention a few highlights. Also, fission of metal clusters has been

covered in great detail in a recent report [4]. The present review will focus on work that has been reported since publication of those earlier reviews [3,4].

2. Rayleigh limit, fission channels, temperature effects and phase transition

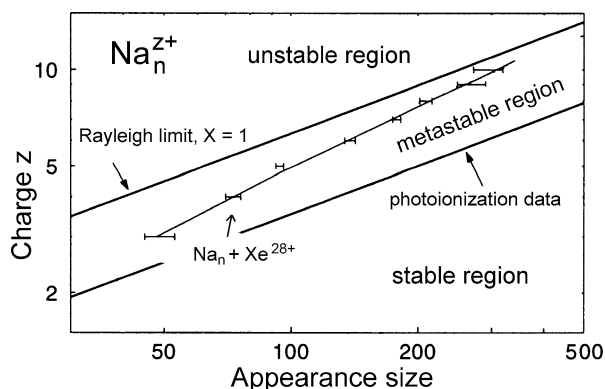
Core excitation of argon clusters by photon absorption is an efficient method to produce doubly charged clusters via the emission of Auger electrons. The fragmentation channels of these systems have been investigated by electron–ion–ion triple coincidence mass spectrometry [5]. The photoelectrons provide the start signal for a time-of-flight mass spectrometer that registers the arrival time, hence mass, of two coincident ions. Even though the average size of the neutral precursors is estimated to be as large as $n \approx 100$, the observed ions are singly charged and surprisingly small, containing just a few atoms. It is found that charged fragments from precursors larger than $n \approx 50$ are not emitted under 180° ; the authors conclude that the picture of electrostatically driven charge separation is inappropriate.

It has been known for some time [6] that, under typical experimental conditions, fission will compete with evaporation of neutral atoms or other building blocks. Hence, the appearance size of cluster ions A_n^{z+} marks the size where, for given z , the two competing processes have equal rates or, approximately, the same activation energies. Clusters A_n^{z+} larger than n_{app} can be observed because monomer evaporation provides an efficient mechanism for cooling, but evaporative cooling below n_{app} will destabilize the cluster with respect to (thermally activated) fission. Hence, n_{app} will be larger than the Rayleigh limit, especially if the multiply charged cluster ions that are prepared in the experiment are vibrationally highly excited. However, theoretical modeling shows that the rates for monomer evaporation and asymmetric fission have different temperature dependences; the cluster size where the two rates are equal will increase with increasing cluster temperature [7].

This effect has been observed in experiments. For example, the appearance size of Na_n^{6+} is 310 ± 10 when large multiply charged sodium cluster ions are ionized and heated by an intense laser at 6.4 eV [8], but the appearance size shifts to 252 ± 8 when Na_n^{6+} is formed by collisions of Na_n with Ar^{8+} at 40 keV [9]. This latter procedure leads, via charge transfer, to relatively cold cluster ions within a very short time (also see Section 6). Fig. 1 compares appearance sizes obtained for Na_n^{z+} with these two experimental methods [10]. The appearance sizes for cluster ions formed by charge transfer in collisions with Xe^{28+} (horizontal bars) are significantly lower than those obtained by photoionization at 6.4 eV (lower solid line). In the former case [10], fissility values reach a maximum of 0.85, for the largest observed charge state of $z = 10$. For photoionization experiments, the fissility parameter amounts to about $X = 0.3$ [8].

However, surprisingly small alkaline earth metal cluster ions, with $z \leq 5$, have been formed by photoionization; their appearance sizes approach the Rayleigh limit [11]. Presumably, fission proceeds via emission of charged monomers rather than small cluster ions such as the trimer that is the favored fragment

Figure 1. Horizontal bars: appearance sizes $n_{\text{app}}(z)$ of Na_n^{z+} , produced by collisions of neutral sodium clusters with Xe^{28+} [10]. The upper solid line indicates the Rayleigh limit (fissility parameter $X = 1$ in Eq. (1)); the lower solid line indicates appearance sizes of Na_n^{z+} obtained by ionization and heating of sodium clusters with an intense pulsed laser at 6.4 eV [8]. Adapted from [10].



ion for multiply charged alkali clusters. Hence, the usual approach of modeling the parent as well as both fragments as metallic droplets is no longer meaningful.

One of the key questions in studies of cluster fission has been the size distribution of fission fragments. There is a marked difference between fission of nuclear systems and of metallic clusters. The former exhibit roughly symmetric fission while the latter exhibit highly asymmetric fission. The difference arises from the difference in charge distribution [7]: nuclei are homogeneously charged while, in metallic clusters, the charge resides on the surface. Fission of nonmetallic clusters, though, may be more symmetric, especially for large sizes, as shown in an experimental study of antimony clusters [12], and a molecular dynamics study of argon clusters [13].

Cluster size and temperature play an important role as well. As noted before, the trimer ion is the preferred light fragment ion in fission of alkali clusters. However, in a recent coincidence study of Na_n^{z+} ($z \leq 5$), formed by collisions with protons at 20 keV, it was found that the trimer ion constitutes only some 70% of all light fragment ions in binary fission events; other light fragment ions range from the monomer to the pentamer [14]. Furthermore, the branching ratio of Na_3^+ versus Na^+ emission increases with increasing parent cluster size. The barrier for fission into Na_3^+ is lower than for fission into Na^+ ; the size dependence of the branching ratio is, accordingly, attributed to a decrease in vibrational temperature with increasing cluster size.

More detailed insight into the competition between different decay channels, and their temperature dependence, requires that the cluster temperature be controlled independently of cluster size. Such a study has been reported for Sr_{19}^{3+} which emits either Sr^+ or Sr_2^+ [15]. The parent ions are formed by photoionization; mass selected ions are then heated by another laser. The temperature can be changed by either changing the photon energy, or the number of absorbed photons. The logarithm of the branching ratio of dimer ion versus monomer ion emission is displayed in Fig. 2, as a function of the inverse cluster temperature. The temperature is varied from 1430 to 2120 K. The data point at $1/(k_B T) \approx 13 \text{ eV}^{-1}$ is obtained from unimolecular decay (without laser heating); it provides an upper limit only. The data are fitted (lines in Fig. 2) by introducing the difference in the fission barriers for the two fission channels, and their differences in entropy, as fit parameters.

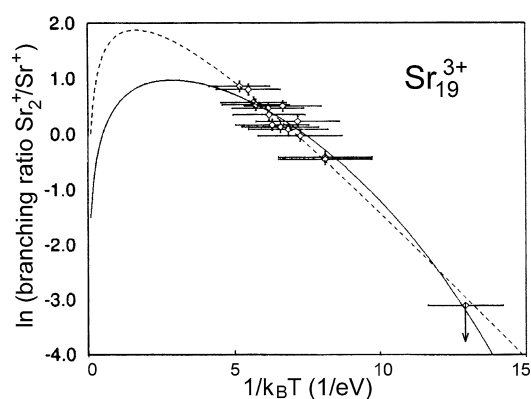


Figure 2. Open dots: experimentally observed branching ratio of two competing fission channels for laser heated Sr_{19}^{3+} , namely ejection of either Sr_2^+ or Sr^+ , as a function of inverse cluster temperature T . Adapted from [15].

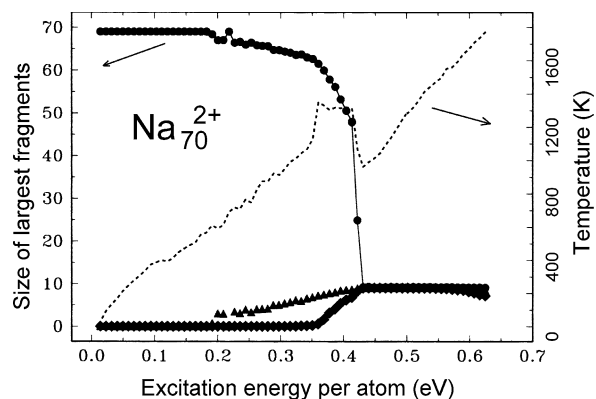
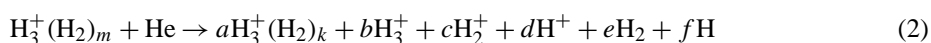


Figure 3. Monte Carlo simulation of a microcanonical ensemble of Na_{70}^{2+} as a function of internal energy E^* per atom. Symbols, together with left ordinate: computed size of the three largest fragments for fission of Na_{70}^{2+} . Dotted line, right ordinate: cluster temperature T as a function of E^* . $T(E^*)$ indicates a first-order phase transition from fission to multifragmentation. Adapted from [16].

In experimental studies of cluster fission, only a narrow range of sizes, charges and temperatures can be studied; theoretical studies do not share this limitation. An exhaustive Monte Carlo investigation of the fission channels of Na_{70}^{z+} has been reported as a function of the internal energy [16]. In Fig. 3 we reproduce the results for $z = 2$. Below internal energies of $E^* = 0.2$ eV per atom only evaporation of neutral monomers is observed; the other fragment is Na_{69}^{2+} (solid diamonds and dots, respectively). Light ions are emitted for higher internal energies (solid triangles). Their size increases gradually with increasing E^* , and they are accompanied by monomer evaporation. A dramatic change occurs above $E^* \approx 0.4$ eV/atom: the size of the largest fragment drops abruptly even though the next largest fragment remains small. This pattern reflects a transition to multifragmentation. The S-shape in the computed $T(E^*)$ curve (dotted line, right ordinate) shows that it is a first order phase transition for the microcanonical ensemble (with a negative heat capacity at the transition), occurring at about 1200 K.

In this context it is interesting to note that one of the great challenges in cluster physics in the last years was the identification and characterization of critical behavior and of phase transitions, including solid-to-liquid and liquid-to-gas phase transitions. Since clusters are particles of finite size, one is confronted with the general question of how to detect and/or characterize such a transition in a finite system, a question of interest for many microscopic or mesoscopic systems such as, for instance, melting and vaporization of metallic clusters, Bose condensation of quantum fluids and nuclear liquid-to-gas transition. One recent successful experimental approach carried out by Gobet et al. [17] involves high-energy collisions (60 keV/amu) of hydrogen cluster ions with a helium target producing also short-lived highly charged hydrogen cluster ions whose decay is then completely analyzed in a recently developed multi-coincidence experiment. Thus they are able to analyze on an event by event basis the identity of all correlated fragments produced in a single collision event between the $\text{H}_3^+(\text{H}_2)_{m \leq 14}$ cluster ion and the He target atom, the fragmentation reactions having the general form



with $a, \dots, f = 0, 1, \dots$. By selecting specific decay reactions they can start after the energizing collision with a microcanonical cluster ion ensemble of fixed excitation energy. From the respective fragment distributions in these decay reactions they derive corresponding temperatures of the decaying cluster ions. The relation between this temperature and the excitation energy (caloric curve) exhibits the typical prerequisites of a first-order phase transition in a finite system, signaling the transition from a bound cluster to the gas phase.

3. Multiply charged fullerene ions

3.1. Multiply charged fullerene cations

The extraordinarily high binding energy of fullerenes [18] makes these molecules perfect candidates for multiple charging. Doubly and triply charged C_{60} ions can be observed rather easily in mass spectra as a result of the low abundance of singly charged fragment ions at this mass per charge range [19]. Fullerenes in charge states higher than 3 often overlap with fragment ions of lower charge states and are difficult to observe. However, in high resolution mass spectrometers isotopomers that contain one or more of the naturally occurring ^{13}C isotopes may be used to uniquely identify higher charge states. Such high resolution mass spectrometry combined with electron impact ionization led to the discovery of multiply charged C_{60}^{z+} up to a charge state of 7 (see Fig. 4) [20]. In addition, the investigation of unimolecular dissociation reactions of multiply charged fullerene ions revealed a novel decay mechanism (in competition to neutral monomer evaporation) where a receding neutral C_2 fragment gets ionized by electron transfer to the highly charged residual fullerene (autocharge transfer reaction [21,22]).

Experiments where highly charged atomic ions are interacting with fullerenes revealed the formation of multiply charged fullerene ions and much less fragmentation compared to electron impact [23]. Thereby it

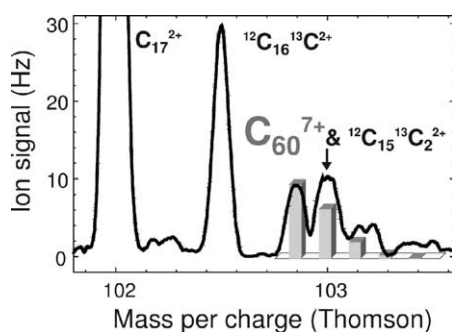


Figure 4. Section of a high resolution mass spectrum of C_{60} showing the details of the identification of the occurrence of C_{60}^{7+} via the corresponding isotomers. Adapted from [20].

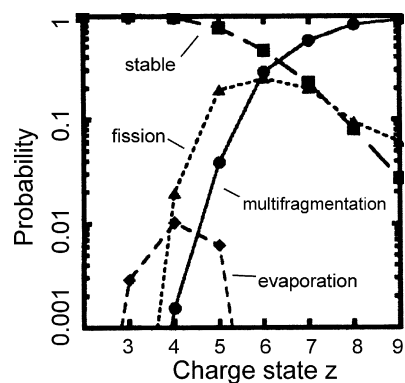


Figure 5. Probabilities of three competing dissociation channels in the reaction $Xe^{30+} + C_{60} \rightarrow Xe^{28+} + C_{60}^{z+*} \rightarrow Xe^{28+} + \text{fragments}$. Adapted from [26].

was possible to observe C_{60}^{z+} ions with z up to 9 [24]. The classical over-the-barrier model that has been developed for the collision of highly charged projectile ions with conducting surfaces has successfully been applied to describe these collision experiments between highly charged ions and fullerenes [25].

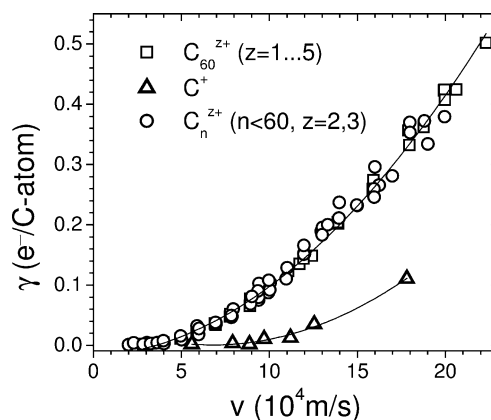
Multi-coincidence techniques have been applied for a complete analysis of all product ions and electrons formed in $Xe^{30+} + C_{60}$ collisions at 300 keV impact energy [26]. These data make it possible to determine the branching ratio between competing reactions, namely formation of stable C_{60}^{z+} , or its decay by evaporation of C_2 , (asymmetric) fission, and multifragmentation, for charge states ranging from $z = 2$ to 9. As shown in Fig. 5, analyzed for reactions that result in Xe^{28+} , evaporation dominates for $z = 3$ [26]. However, as z increases, fission quickly takes over because the fission barrier decreases with increasing z . Beyond $z = 6$ multifragmentation, i.e. the complete destruction of C_{60} into small fragment and fragment ions, dominates.

Multiphoton ionization with picosecond laser pulses leads to strong fragmentation and delayed electron emission, but not to the formation of multiply charged fullerenes [27]. On the other hand, single photon ionization using synchrotron light leads to similar results as electron impact [28], i.e., moderate fragmentation and some highly charged fullerene ions. However, if the length of a laser pulse is shortened from ps to fs the resulting mass spectra change dramatically [29]. With the right conditions for the wavelength and duration of the laser pulse, up to 10 electrons have been removed from C_{60} , and the resulting ion C_{60}^{10+} has been identified mass spectrometrically [30]. The strong electromagnetic field of the laser light has a similar effect on the fullerenes as the Coulomb field of a highly charged atomic ion that leads to the soft removal of many electrons without strongly exciting the vibrational modes (also see Section 6 of this review).

3.2. Fullerene dianions

Hettich et al. [31] and Limbach et al. [32] reported the observation of long-lived doubly charged negative ions of C_{60} and C_{70} in the gas phase. These dianions were generated by laser desorption from a surface covered with fullerenes and are believed to be produced by negative surface ionization from the laser-heated surface. The first group extended their work on dianions to highly fluorinated $C_{60}F_{48}$. Sequential attachment of two electrons to highly fluorinated $C_{60}F_{48}$ in the gas phase produced $C_{60}F_{48}^{2-}$ and $C_{60}F_{46}^{2-} + F_2$ [33]. The dianion $C_{60}F_{48}^{2-}$ was found to be more stable with respect to electron detachment than the corresponding singly charged anion. Like in the case of the fluorinated C_{60} , the larger fullerene C_{84} allows sequential attachment of two electrons in the gas phase [34].

Figure 6. Total electron yields γ versus impact velocity v for impact of differently charged C_n^{z+} ions ($z = 1-5$, $n \leq 60$) on clean polycrystalline gold. Also shown is, for comparison, the yield for atomic carbon ions. Adapted from [36].



3.3. Reactions of multiply charged fullerenes

Reactions have been studied in gas-phase as well as surface collisions. Bohme and coworkers investigated ion molecule reactions of fullerene ions up to charge state 3 in a selected ion flow drift tube [35]. Measured rate coefficients and observed product channels for reactions with a variety of inorganic and organic molecules depend strongly on the charge state of C_{60} . Measured rate coefficients span more than 4 orders of magnitude. Product channels observed include attachment, dissociative attachment, dissociative attachment with charge separation, single-electron transfer, dissociative single-electron transfer, two-electron transfer and a novel type of polymerization driven by the multiply charged fullerene ion.

The electron emission statistics upon collision of C_n^{z+} ions ($n \leq 60$ and $z \leq 5$) onto clean polycrystalline gold surfaces has been measured by Winter et al. [36]. At a given impact energy, there is a linear dependence of electron yield on carbon cluster size. However, there is no influence of the projectile charge and, thus, apparently no potential electron emission, in striking contrast to the impact of slow multiply charged atomic ions on solid surfaces (see Fig. 6). This suppression of potential emission can be attributed to a rapid transfer of the fullerene electronic excitation, gained during surface neutralization, to projectile vibrational degrees of freedom and subsequent fast fragmentation. Molecular dynamics calculations show that this fragmentation takes place within picoseconds after surface impact, much faster than the established rates for thermionic electron emission from collisionally heated fullerenes. In an extension to these electron emission studies [36], Biasioli et al. [37] investigated the scattered product ions formed upon the collision of singly and multiply charged ions C_{60}^{z+} ($z = 1$ to 5) with a hydrocarbon-covered stainless steel surface. All ions scattered off the surface are singly charged. The extent of fragmentation increases with the collision energy and the projectile charge. However, the increase of fragmentation with the charge of the projectile is less pronounced than expected from a full conversion of electronic energy, gained in the neutralization process, into internal energy of the ion.

4. Highly charged, micrometer-sized particles suspended in ion traps

Ion traps make it possible to monitor the size and charge of very large droplets over hundreds of seconds. In a series of experiments, highly charged droplets of glycol with a radius of the order of $r = 10 \mu\text{m}$ were monitored while they slowly evaporated neutral molecules; a dry buffer gas made sure that the temperature of the evaporating droplets remained constant [38]. The angular distribution of Mie-scattered laser light was used to measure the temporal evolution of the droplet radius; at the same time the charge-to-mass ratio of the droplet was determined from the dc bias voltage that was required to compensate for the gravitational force and to keep the droplet in the center of the ion trap.

As the droplet shrinks in size while its charge, of the order of 1 pC, remains constant, its fissility parameter increases. As shown in Fig. 7, a succession of several distinct Coulomb explosions is observed as

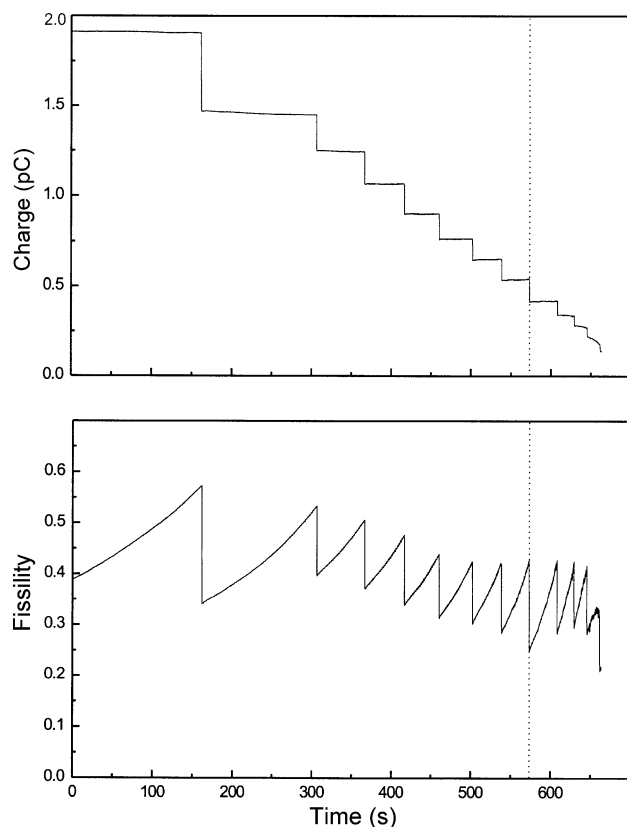


Figure 7. Temporal evolution of net charge and fissility of positively charged glycol droplets, suspended in an ion trap.

For most of the time, the droplet is evaporating neutral molecules; its charge remains constant (upper panel) while its fissility increases (lower panel). Discontinuities indicate the occurrence of

Coulomb explosion, the ejection of highly charged, small amounts of matter.

Adapted from [38].

the droplet shrinks in size from, typically, 30 to 10 μm . For each explosion, the mass decreases by no more than a few percent. Coulomb explosion seems to occur for fissility parameters as small as 0.5. However, a number of factors may explain this result. For example, the scattering patterns indicate that explosion is preceded by strong surface oscillations of the droplets. Moreover, the values that are assumed in the analysis for the surface tension and the index of refraction may be in error due to finite-size corrections, and because small amounts of impurities will, as the droplet shrinks, become enriched; this may lead to erroneous calculations of r and X .

5. Multiply charged cluster anions

Multiply charged anions are common in the condensed phase but, until recently, they were rarely observed in the gas phase. This has changed dramatically within the last decade [39]. Dianions often feature a very large repulsive Coulomb barrier towards electron emission, caused by the short-range attraction of the electron with the nuclei, and the long-range repulsion between the emitted electron and the remaining anion [40]. The barrier and the second electron affinity can be probed by photon electron spectroscopy, PES. Wang et al. have applied PES to a large number of molecular dianions and a few small cluster dianions (see [41] for a review). It was observed that dianions may have lifetimes exceeding hundreds of seconds even when the second electron affinity of the molecule is negative by 0.9 eV, i.e. when electron detachment from the dianion is exoergic by 0.9 eV.

One of the first cluster dianions to be observed were small carbon clusters. Their linear structure reduces the Coulomb repulsion. C_8^{2-} , which has been observed, is believed to be stable [40]. Likewise, mixed $\text{Si}_x\text{C}_y^{2-}$ dianions in this size range may be stable with respect to autodetachment although linear structures

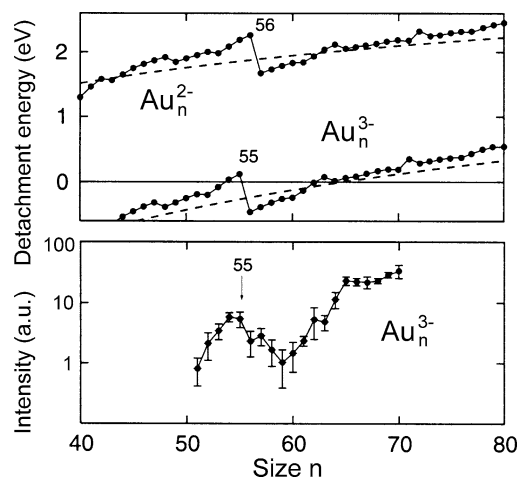
are not necessarily the ones with the longest lifetime [42]. Fullerene dianions have been discussed in a previous section of this review. The Coulomb explosion imaging technique has been used to identify MgF_4^{2-} [43].

We now turn to metal cluster anions. Given that these systems can be made arbitrarily large, it may seem surprising that no metal cluster dianions had been observed until very recently. Kappes and coworkers identified Pb_n^{2-} with $n \geq 35$ and Pb_n^{3-} with $n \geq 76$ in the plume created by laser ablation of lead [44]. Schweikhard and coworkers were able to form silver cluster dianions and gold cluster di- and trianions by irradiating trapped, singly charged cluster anions with an intense beam of low-energy electrons [45,46]. The appearance size of Au_n^{2-} was 12, significantly smaller than the value $n_{\text{app}} = 29$ that was obtained from laser ablation of gold which will lead to vibrationally hot cluster ions [44]. The intensities of these dications show anomalies that agree with predictions of the spherical jellium model. For example, relatively high intensities are observed for $n = 16$ and 18, which correspond to shell closures at $n_e = 18$ and 20 electrons. A more quantitative comparison has been presented based on a finite-temperature semi-empirical shell-correction method [47]. The computed second electron affinities track very closely the abundance of the observed ions; Au_{12}^{2-} is, indeed, the smallest dication that is stable with respect to electron detachment. Likewise, excellent agreement between experimental abundances and computed third electron affinities is obtained for Au_n^{3-} [46]. Fig. 8 shows, in the upper panel, second and third electron affinities of gold clusters, computed by a finite-temperature shell-correction method, while the abundance of Au_n^{3-} , experimentally observed in an ion trap, is displayed in the lower panel [46]. Note the local enhancement of Au_{55}^{3-} in the experimental and theoretical data which arises from a major electronic shell closure when the number of valence electrons is $n_e = 55 + 3 = 58$.

In this latter work [46], the decay channels were considered as well. Multiply charged anions may reduce their charge either by autodetachment or, like their positively charged counterparts, by fission. If fission were the dominating decay channel for anions, then their appearance size would be expected to agree, approximately, with those of cations, except for a slight systematic shift due to electronic shell effects. However, the experimental appearance sizes are $n_{\text{app}}(z = 3) = 16$ for cations, and 51 for anions. Computations do, indeed show that Au_n^{3-} is stable with respect to fission for $n \geq 25$ (the fission barrier would reduce the appearance size even further), but they are not stable with respect to autodetachment unless $n \geq 54$. Hence, the stability limit of multiply charged gold cluster anions is dictated by autodetachment, not by fission.

This need not be universally true. For example, doubly charged metal tetrahalides appear to be metastable with respect to loss of halide anions, rather than autodetachment [48].

Figure 8. Upper panel: computed second and third electron affinities of Au_n . Lower panel: abundance of Au_n^{3-} observed in a Penning ion trap. Adapted from [46].



6. Coulomb explosion driven by intense, ultrafast laser pulses or by collisions with highly charged ions

The interaction of intense laser pulses of sub-picosecond duration with free van der Waals and metal clusters causes multielectron dissociative ionization that has a number of remarkable consequences: emission of highly charged ions with large kinetic energies, and emission of bright X-rays in the range of 0.1 to 5 keV. Although some of these phenomena have been observed before in the interaction of intense lasers with either atoms and small molecules, or with solids, the mechanism of laser interaction with clusters has distinct features. Moreover, in contrast to laser interaction with solid targets, a cluster target avoids one of the problems common to solid targets: clusters can be easily and continuously replenished in a beam. For a recent review, see [49].

The absorption of laser light in moderately dense cluster beams (10^{19} atoms/cm³) can reach 100%, resulting in the absorption of about 1 keV per atom. In early experiments, emission of hard X-rays from laser-excited rare gas clusters was attributed to the creation of ‘hollow atoms’ that have several inner-shell vacancies [50]. For Kr clusters irradiated by laser intensities of $5 \cdot 10^{17}$ W/cm² in the IR, a yield of $4 \cdot 10^6$ X-ray photons per laser shot, primarily L_α and L_β , has been measured [51]. In other early work, ions as highly charged as I^{17+} and Ar^{8+} were observed in experiments with $(HI)_n$ and $(HI)_n Ar_m$ clusters; their kinetic energies were found to increase with charge state and reached values of several hundred eV for $z = 7$. In experiments on platinum clusters, the value of z was shown to increase strongly when the laser pulse was lengthened while keeping the laser pulse energy constant [52]. In recent work, ions as highly charged as Xe^{40+} , with kinetic energies up to 1 MeV, have been identified [53,54].

Kinetic energies are much lower when clusters of light elements are irradiated. Still, irradiation of deuterium cluster beams has been shown to result in the emission of 2.45 MeV neutrons which signal the occurrence of fusion reactions between energetic deuterons [55]:



A maximum yield of 10^4 neutrons per laser pulse was observed when the size of $(D_2)_n$ clusters, determined by Rayleigh scattering, averaged 50 Å. The yield of neutrons may be further enhanced if cluster targets are used that also involve heavier elements, such as $(D_2O)_n$, because the larger inertial confinement and the larger attainable charge states will lead to higher kinetic energies of the deuterons [56]. These results offer the exciting possibility of creating bright pulses of nearly monoenergetic neutrons with sub-nanosecond pulse durations in a table-top experiment.

Several models have been proposed to account for the observations described above [57–60]. Not any one of them may be able to account for all experimental observations under the various experimental conditions (i.e., duration and power density of the laser pulse, size of the clusters, and their composition). One of these models, based on classical molecular dynamics simulations of large xenon clusters [60], separates the dynamics of laser-irradiated clusters into several steps: within a few fs, almost all of the (eight) outer-shell electrons are removed from the xenon atoms under the influence of the laser field which is of the order of 10 V/Å. The free electrons resulting from this ‘inner ionization’ form a dense plasma with a non-uniform charge distribution that generates an inner electric field and further enhances the inner ionization, leading to the rapid removal of more strongly bound $4d$ -electrons. Unbound electrons gradually leave the cluster (‘outer ionization’) which results in a net charge of the cluster and an increase in its ionization energy which limits the rate at which outer ionization occurs. The unbound electrons may oscillate under the influence of the electric field and undergo frequent collisions for quite a while. After a few tens of fs, the size of the highly charged cluster begins to increase quickly. This weakens the inner fields and leads to large-amplitude oscillation of the electrons in phase with the electric field, quasiresonant absorption of energy, and rapid ejection of most unbound electrons. Ultimately, Coulomb explosion will lead to atomic ions that are, on average, 10-fold charged and carry a kinetic energy of several tens of keV.

Collisions of fast, highly charged atomic ions with clusters also lead to intermediate, highly charged systems on the time scale of a few femtoseconds. Results pertaining to metal clusters and fullerenes have been discussed above (see Sections 2 and 3). Depending on the conditions, the system may completely disintegrate but, in contrast to excitation by femtosecond lasers, highly charged atomic ions are rarely observed. However, collisions of argon clusters with highly charged Xe ions result in atomic argon ions in charge states as high as $z = 8$ [61]. The difference is attributed to charge localization: in fullerenes and metal clusters, the charges that may initially be localized on one atom can equilibrate over the cluster within a fraction of a picosecond, before Coulomb explosion can take place, while they remain localized in argon clusters. This result differs from that following core-level excitation of argon clusters [5], described earlier in this review.

7. Conclusions

A decade ago the basic mechanism of Coulomb explosion of atomic clusters seemed to be reasonably well understood. A large body of data had been collected, and systematic trends became apparent. However, the introduction of novel experimental approaches during the past decade has greatly enhanced our understanding of Coulomb explosion. Most notable among them are multi-coincidence techniques, ion trapping, heating or cooling multiply charged cluster ions, preparing them with low excess energy by charge transfer collisions, and interaction of clusters with femtosecond laser pulses. So far, most of these techniques have been applied to just a few systems, with fullerenes and monovalent metal clusters having received the greatest attention. There is little doubt that the application of novel techniques to other types of clusters will continue to reveal new and surprising features of the phenomenon of Coulomb explosion.

Acknowledgements. Work supported by FWF, ÖAW and ÖNB, Wien, and EU Commission, Brussels.

References

- [1] L. Rayleigh, *Philos. Mag.* A 14 (1882) 184.
- [2] K. Sattler, J. Mühlbach, O. Echt, P. Pfau, E. Recknagel, *Phys. Rev. Lett.* 47 (1981) 160.
- [3] O. Echt, T.D. Märk, in: H. Haberland (Ed.), *Clusters of Atoms and Molecules II*, Vol. 56, Springer-Verlag, Berlin, 1994, p. 183.
- [4] U. Näher, S. Bjornholm, S. Frauendorf, F. Garcias, C. Guet, *Physics Reports-Review Section of Phys. Lett.* 285 (1997) 245.
- [5] E. Rühl, C. Heinzl, H. Baumgartel, M. Lavollee, P. Morin, *Z. Phys. D* 31 (1994) 245.
- [6] W.A. Saunders, *Phys. Rev. A* 46 (1992) 7028.
- [7] P. Fröbrich, *Ann. Phys.* 6 (1997) 403.
- [8] U. Näher, S. Frank, N. Malinowski, U. Zimmermann, T.P. Martin, *Z. Phys. D* 31 (1994) 191.
- [9] F. Chandezon, C. Guet, B.A. Huber, D. Jalabert, M. Maurel, E. Monnard, C. Ristori, J.C. Rocco, *Phys. Rev. Lett.* 74 (1995) 3784.
- [10] F. Chandezon, S. Tomita, D. Cormier, P. Grübling, C. Guet, H. Lebius, A. Pesnelle, B.A. Huber, *Phys. Rev. Lett.* 87 (2001) 153402.
- [11] M. Heinebrodt, S. Frank, N. Malinowski, F. Tast, I.M.L. Billas, T.P. Martin, *Z. Phys. D* 40 (1997) 334.
- [12] C. Brechignac, P. Cahuzac, F. Carlier, M. Defrutos, J. Leygnier, J.P. Roux, *J. Chem. Phys.* 102 (1995) 763.
- [13] A. Goldberg, I. Last, T.F. George, *J. Chem. Phys.* 100 (1994) 8277.
- [14] F. Chandezon, T. Bergen, A. Brenac, C. Guet, B.A. Huber, H. Lebius, A. Pesnelle, *Phys. Rev. A* 6305 (2001) 1201.
- [15] C. Brechignac, P. Cahuzac, N. Kebaili, J. Leygnier, *Phys. Rev. Lett.* 81 (1998) 4612.
- [16] O. Schapiro, P.J. Kuntz, K. Mohring, P.A. Hervieux, D.H.E. Gross, M.E. Madjet, *Z. Phys. D* 41 (1997) 219.
- [17] F. Gobet, B. Farizon, M. Farizon, M.J. Gaillard, J.P. Buchet, M. Carre, T.D. Märk, *Phys. Rev. Lett.* 87 (2001) 203401.
- [18] S. Matt, O. Echt, P. Scheier, T.D. Märk, *Chem. Phys. Lett.* 348 (2001) 194.
- [19] C.W. Walter, Y.K. Bae, D.C. Lorents, J.R. Peterson, *Chem. Phys. Lett.* 195 (1992) 543.
- [20] P. Scheier, T.D. Märk, *Phys. Rev. Lett.* 73 (1994) 54.
- [21] P. Scheier, B. Dünser, T.D. Märk, *Phys. Rev. Lett.* 74 (1995) 3368.
- [22] P. Scheier, B. Dünser, T.D. Märk, *J. Phys. Chem.* 99 (1995) 15428.
- [23] B. Walch, C.L. Cocke, R. Voelpel, E. Salzborn, *Phys. Rev. Lett.* 72 (1994) 1439.

- [24] J. Jin, H. Khemliche, M.H. Prior, Z. Xie, *Phys. Rev. A* 53 (1996) 615.
- [25] U. Thumm, A. Barany, H. Cederquist, L. Hagg, C.J. Setterlind, *Phys. Rev. A* 56 (1997) 4799.
- [26] S. Martin, L. Chen, A. Denis, R. Bredy, J. Bernard, J. Desesquelles, *Phys. Rev. A* 62 (2000) 022707.
- [27] P. Wurz, K.R. Lykke, *J. Chem. Phys.* 95 (1991) 7008.
- [28] H. Steger, J. deVries, B. Kamke, W. Kamke, T. Drewello, *Chem. Phys. Lett.* 194 (1992) 452.
- [29] E.E.B. Campbell, K. Hansen, K. Hoffmann, G. Korn, M. Tchapyguine, M. Wittmann, I.V. Hertel, *Phys. Rev. Lett.* 84 (2000) 2128.
- [30] D.M. Rayner, unpublished, 2002.
- [31] R.L. Hettich, R.N. Compton, R.H. Ritchie, *Phys. Rev. Lett.* 67 (1991) 1242.
- [32] P.A. Limbach, L. Schweikhard, K.A. Cowen, M.T. McDermott, A.G. Marshall, J.V. Coe, *J. Am. Chem. Soc.* 113 (1991) 6795.
- [33] C. Jin, R.L. Hettich, R.N. Compton, A. Tuinman, A. Derecskei-Kovacs, D.S. Marynick, B.I. Dunlap, *Phys. Rev. Lett.* 73 (1994) 2821.
- [34] R.N. Compton, A.A. Tuinman, C.E. Klots, M.R. Pederson, D.C. Patton, *Phys. Rev. Lett.* 78 (1997) 4367.
- [35] Y. Ling, G.E. Koyanagi, D. Caraiman, A.C. Hopkinson, D.K. Bohme, *Int. J. Mass Spectrom. Ion Proc.* 192 (1999) 215.
- [36] H.P. Winter, M. Vana, G. Betz, F. Aumayr, H. Drexel, P. Scheier, T.D. Märk, *Phys. Rev. A* 56 (1997) 3007.
- [37] F. Biasioli, T. Fiegele, C. Mair, Z. Herman, O. Echt, F. Aumayr, H.P. Winter, T.D. Märk, *J. Chem. Phys.* 113 (2000) 5053.
- [38] D. Duft, Diploma Thesis, Freie Universität Berlin, Berlin, 1999.
- [39] M.K. Scheller, R.N. Compton, L.S. Cederbaum, *Science* 270 (1995) 1160.
- [40] A. Dreuw, L.S. Cederbaum, *Phys. Rev. A* 6301 (2001) 2501.
- [41] L.S. Wang, X.B. Wang, *J. Phys. Chem.* 104 (2000) 1978.
- [42] A. Dreuw, T. Sommerfeld, L.S. Cederbaum, *J. Chem. Phys.* 109 (1998) 2727.
- [43] R. Middleton, J. Klein, *Phys. Rev. A* 60 (1999) 3515.
- [44] C. Stoermer, J. Friedrich, M.M. Kappes, *Int. J. Mass Spectrom.* 206 (2001) 63.
- [45] L. Schweikhard, A. Herlert, S. Kruckeberg, M. Vogel, C. Walther, *Philos. Mag. B* 79 (1999) 1343.
- [46] C. Yannouleas, U. Landman, A. Herlert, L. Schweikhard, *Phys. Rev. Lett.* 86 (2001) 2996.
- [47] C. Yannouleas, U. Landman, *Phys. Rev. B* 61 (2000) R10587.
- [48] P. Weis, O. Hampe, S. Gilb, M.M. Kappes, *Chem. Phys. Lett.* 321 (2000) 426.
- [49] J.H. Posthumus, in: *Molecules and Clusters in Intense Laser Fields*, Cambridge University Press, 2001, p. 272.
- [50] A. McPherson, B.D. Thompson, A.B. Borisov, K. Boyer, C.K. Rhodes, *Nature* 370 (1994) 631.
- [51] S. Dobosz, M. Lezius, M. Schmidt, P. Meynadier, M. Perdrix, D. Normand, *Phys. Rev. A* 56 (1997) R2526.
- [52] L. Koller, M. Schumacher, J. Kohn, S. Teuber, J. Tiggesbaumker, K.H. Meiwes-Broer, *Phys. Rev. Lett.* 82 (1999) 3783.
- [53] T. Ditmire, J.W.G. Tisch, E. Springate, M.B. Mason, N. Hay, J.P. Marangos, M.H.R. Hutchinson, *Phys. Rev. Lett.* 78 (1997) 2732.
- [54] M. Lezius, S. Dobosz, D. Normand, M. Schmidt, *Phys. Rev. Lett.* 80 (1998) 261.
- [55] J. Zweiback, T.E. Cowan, R.A. Smith, J.H. Hartley, R. Howell, C.A. Steinke, G. Hays, K.B. Wharton, J.K. Crane, T. Ditmire, *Phys. Rev. Lett.* 85 (2000) 3640.
- [56] I. Last, J. Jortner, *Phys. Rev. Lett.* 87 (2001) 033401.
- [57] A.B. Borisov, J.W. Longworth, A. McPherson, K. Boyer, C.K. Rhodes, *J. Phys. B* 29 (1996) 247.
- [58] C. Wülker, W. Theobald, D. Ouw, F.P. Schaäfer, B. Chichkov, *Opt. Commun.* 112 (1994) 21.
- [59] T. Ditmire, *Phys. Rev. A* 57 (1998) R4094.
- [60] I. Last, J. Jortner, *Phys. Rev. A* 6201 (2000) 3201.
- [61] W. Tappe, R. Flesch, E. Rühl, R. Hoekstra, T. Schlathölter, *Phys. Rev. Lett.* 88 (2002) 143401.